JOURNAL OF MATERIALS SCIENCE 15 (1980) 345–352

Single particle impact damage of fused silica

M. M. CHAUDHRI, PATRICIA A. BROPHY
Physics and Chemistry of Solids, Cavendish Laboratory, Madingley Road, Cambridge, UK

Single-impact damage of fused silica by spherical and conical tungsten carbide (WC) projectiles of velocities up to 200 m sec^{-1} has been investigated with a high-speed framing camera photographing at a rate of up to 1.7 x 10^6 frames per second. For spherical particles the Hertzian cone cracks, which for higher impact velocities are accompanied by median and radial cracks, form during the loading part of the impact; some growth of all these cracks also occurs during unloading. With the conical particles the Hertzian cone cracks do not form; only radial and median cracks form during the loading; in this case both radial and median cracks grow during the unloading. In both cases "lateral" cracks form during unloading. From these experiments values of the static equivalent of the dynamic stress-intensity factor for high-velocity cracks are also obtained; these are found to be considerably lower than those obtained from quasi-static indentation experiments. Finally, the extent of the damage produced by a single impact has been discussed.

1. Introduction

Damage of highly brittle materials by the impact of small "blunt" and "sharp" particles is of considerable academic and practical interest. We have recently examined with high-speed framing microphotography (framing rates up to ~ 2 x 10^6 sec^{-1}) the response of soda lime and borosilicate glasses [1–3], and ionic crystals [4] to small spherical particle impacts. It was noted that unlike the quasi-static case, the crack velocity in the material plays a significant role in controlling the extent of the damage [3]. For example, the length of the Hertzian cone crack in borosilicate glass, which has a significantly higher maximum crack velocity, is about 1.5 to 2 times that in soda-lime glass under similar impact conditions. Furthermore, unlike the quasi-static case, "lateral"* cracks can also form without any plastic/permanent deformation of the impacted surface [3]. To illustrate this a sectioned view of damage in soda-lime glass by the impact of a 1 mm diameter hardened steel ball at a velocity of 120 m sec^{-1} is shown in Fig. 1 which reveals the turning up of the tip of the cone crack towards the impacted surface; this is in the absence of any permanent deformation; at slightly higher speeds these cracks would come up to the impacted surface thus causing loss of material from the surface.

It has been suggested by some authors that the extent of the cracks produced in a brittle solid by particle impact can be predicted from fracture parameters obtained from standard quasi-static indentation tests [8, 9]; by measuring the loss of the strength of the impacted surface they found an agreement with the predictions. However, it is pointed out that the strength measurements manifest the square root of the crack lengths and therefore any discrepancies between the experimental findings and theoretical predictions are correspondingly reduced and thus may go unnoticed. We therefore hold that the direct measurements (with optical and/or X-ray techniques) of the extent of the cracks is a more reliable and satisfactory method for checking the predictions of any theories.

The purpose of this investigation was to extend

* This crack system in brittle materials was observed to form when they were quasi-statically indented with Vickers diamond pyramids in earlier studies of Taylor [5] and Mulhearn [6]. These investigators explained the formation of these cracks on the relaxation of the residual stresses in material about the indentations after the removal of the indentation load. Further extension of these ideas, especially in connection with the removal of surface material, has been made by Lawn and co-workers (see [7]).

0022–2461/80/020345–8$02.80/0

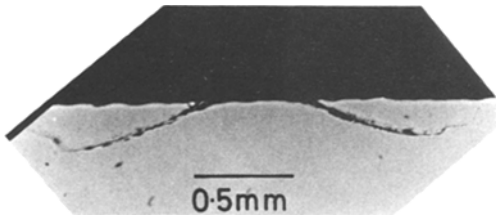

Figure 1 Sectioned and etched view of the damage in soda-lime glass by the impact of a 1 mm diameter hardened steel sphere at a velocity of 120 m sec^{-1}. Note the edges of the cone crack turn up towards the impacted surface without their being any permanent deformation where the impact occurred.

the particle impact experiments to fused silica, especially as this relatively open-structured material, unlike soda-lime glass, undergoes pronounced permanent densification [10, 11] during a static indentation, which can lead to the formation of the Hertzian cone cracks even with Vickers diamond pyramids [12]. Here both spherical and pointed projectiles have been used, and quite distinct differences have been found in the nature of the damage in the two cases.

2. Experimental procedure

Annealed blocks of pure fused silica (Vitreosil; Thermal Syndicate Ltd) of size 50 mm × 25 mm × 10 mm and polished to optical quality surfaces were used. The projectiles were 1 mm diameter tungsten carbide spheres and cones with semi-apical angle of $\pi/4$, base of radius 0.5 mm, and the radius of the apex less than 5 μm. Using an explosively driven gun the particles were projected normally at a velocity in the range 100 to 200 m sec^{-1} on to a large face of the block which was acoustically matched to another block so as to minimize the intensity of the reflected stress waves returning to the damage site. The entire event was photographed with a rotating mirror framing camera using back lighting as described elsewhere [1]. Crack-velocity measurements from the photographic sequences had an error of less than 5%. The damage was further examined by sectioning the specimen followed by mechanical polishing and a light etch in diluted hydrofluoric acid. In another series of experiments the specimens were quasi-statically indented with Vickers diamond pyramids, and the extent of the median cracks was measured for different loads.

3. Results

3.1. Spherical particle impacts

The Hertzian cone crack formed for all velocities above 10 m sec^{-1}, and at velocities greater than 150 m sec^{-1} several cone, radial, median and lateral cracks formed. At a framing speed of 1.7×10^6 sec^{-1} it was found very difficult to synchronize the camera with the event for low impact velocities. Therefore most of the photographic work was done at velocities greater than 100 m sec^{-1}. A typical sequence is shown in Fig. 2. A 1 mm diameter WC sphere moving at 200 m sec^{-1} has just made contact in frame 3, but no cracks have been initiated. In the next frame the sphere has gone into the material by 110 μm (it is assumed here that as the WC sphere is much harder than fused silica it does not deform and, in fact, examination of the sphere after the impact revealed no permanent deformation), and two cone cracks of different semi-apical angles, 39° and 47°, but having the same axis are initiated at the contact circle. (Higher magnification sequences have shown that, as in the quasi-static case, the cone crack initiates from just outside the contact circle.) It is not clear in this frame whether any radial or median cracks have formed, but in the next frame a well-developed semi-circular shaped median crack is present and the extent of the cone cracks has increased (the damage with high-velocity WC spheres is so severe that the appearance of the cone cracks, especially during the early stages of their growth is less smooth than in the case of steel or glass spheres impacting at even up to 350 m sec^{-1}). The velocity of the cone and median cracks is 2500 m sec^{-1}; the value of the maximum crack velocity from several experiments is found to be 2350 ± 40 m sec^{-1}, which is ~ 10% higher than the maximum crack velocity in fused silica as measured by Schardin [13] and Field [14]. It will be seen that on the left of the sphere a small protrusion (due to the debris coming up) exists, while the sphere has gone into the material by 150 μm. In frame 6 this debris, D, is quite distinct and its velocity is 550 m sec^{-1}; the median, M, and cone cracks have grown further, but the particle has started to rebound as its penetration into the material is now ~ 130 μm. However, as the intensity of the transmitted light is not enough we cannot say whether any lateral cracks have formed at this stage of unloading. The unloading continues in frame 7, but both the median and the inner cone cracks still grow, though only by small

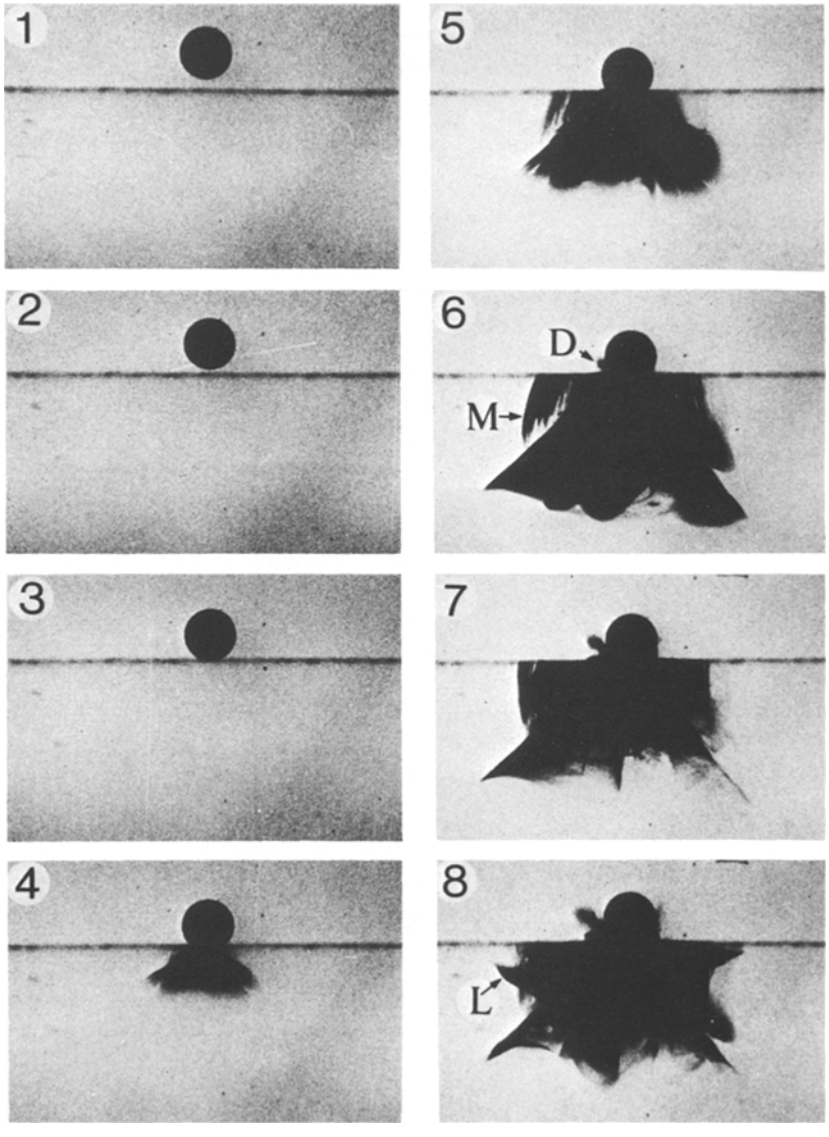

Figure 2 Impact of a 1 mm diameter tungsten carbide sphere on a block of fused silica at a velocity of 200 m sec^{-1}. Cone, and median, M, cracks form during loading and continue to grow during unloading, whereas the laterial cracks are initiated only during unloading. Interframe time: 0.6 μsec.

amounts. A lateral crack which appears on the left of the cone cracks, becomes more pronounced in frame 8 (see at L); another well-formed lateral crack will be seen on the right of the cone cracks. The median and the cone cracks do not grow any more between frames 7 and 8. The sphere leaves the surface in the next frame (not shown); this is accompanied by a very slight turning up of the tip of the inner cone crack and the further extension of the lateral cracks. A sectioned view of the damage site (Fig. 3) shows that the prominent lateral cracks originate at the skirts of the cone cracks, an observation also made from earlier dynamic [3] and static studies [12].

3.2. Cone impacts

Our main aim in these experiments was to study the impact of the apex of the cone with the cone axis being normal to the silica block surface. Several attempts failed to achieve such impact conditions as the cone usually tilted during its 11 mm flight. Nevertheless, the best sequence obtained so far is shown in Fig. 4. The cone impacts between frames 1 and 2 at a velocity of

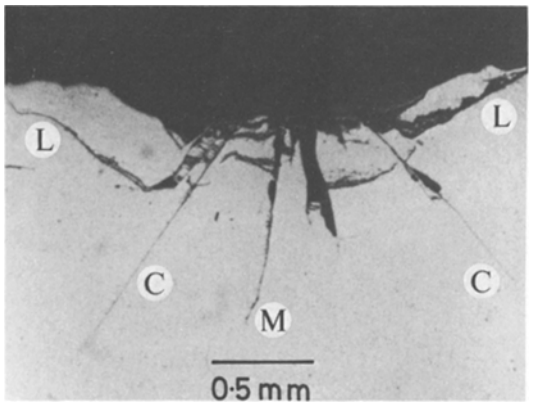

Figure 3 Sectioned and etched view of the damage shown in Fig. 2. Note the semi-apical angle of the inner cone crack CC is 47°, which is considerably smaller than the value of 65.5° as found by Benbow [15] for the case of quasi-static loading; cone angle versus impact velocity has been discussed elsewhere [2]. A considerable amount of lateral cracking LL is initiated at the skirts of the cone cracks. M is the median crack.

170 m sec^{-1}. In frame 2 a median crack (full disc) has appeared from near the tip of the projectile; the crack velocity is at least 2500 m sec^{-1}. In the next frame the crack spreads to the impacted surface and now it is a well-developed semi-circular disc, the velocity reducing to 1400 m sec^{-1}. The projectile rebound starts to occur between frames 3 and 4 but the median crack, M, grows further at an average velocity of 950 m sec^{-1}. A prominent lateral crack can also be seen to be forming at the left of the projectile. As the rebound continues, further growth of this lateral crack occurs, though some new lateral cracks also form. However, there is no growth of the median crack after frame 4; some material is removed from the surface in the form of fine debris, which is ejected at a velocity 3 times the impact velocity. The top and sectioned views of the damage are shown in Fig. 5a and b, respectively. Note that unlike the case of quasi-static indentations with Vickers diamond pyramids

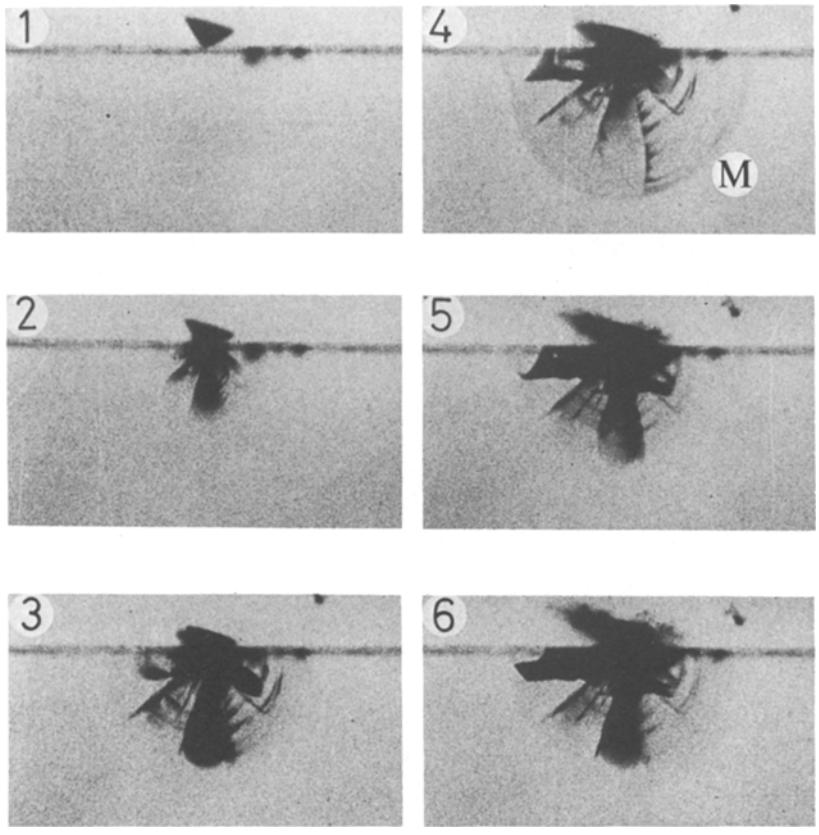

Figure 4 Impact of a tungsten carbide cone of semi-apical angle $\pi/4$ and base diameter 1 mm on a block of fused silica at 170 m sec^{-1}. No cone cracks form and a well developed median crack of half penny shape is shown at M in frame 4. Interframe time: 0.6 μsec.

[12], the Hertzian cone cracks do not form in these impact experiments.

3.3. Quasi-static indentations

Vickers diamond pyramid indentations were made for loads up to 400 N on the as-received surface of 6 mm thick fused silica plates using a heavy duty Vickers machine. At these loads quite distinct median cracks were formed whose extent grew with the applied load. From such experiments fracture surface energy can be easily obtained and this technique has been widely used for a wide range of materials from silicate glasses and ceramics [7] to explosive crystals [16]. A plot of load versus (crack length)$^{3/2}$ for our fused silica experiments is a straight line (Fig. 6) from which a value of 1.45×10^6 N m$^{-3/2}$ for the static critical stress-intensity factor is obtained. Using Equation 1 (see later) and taking $E = 7.25 \times 10^{10}$ N m^{-2} and $\nu = 0.17$ we obtain the fracture surface energy, $\gamma = 14.1$ J m^{-2}. This is higher than the value of 3.48 J m^{-2} obtained by Wiederhorn [17] using the double-cantilever cleavage technique, but approximately agrees with 9 J m^{-2} obtained by Kendall [18] using the technique of compression cracking; this difference between our and Kendall's values and those of Wiederhorn may be due to the work involved in compacting the material.

Similar indentations for similar range of loads were made on plates of soda-lime glass as well, and it was found that for a given load the length of the median crack in this glass was up to 3 times that in fused silica.

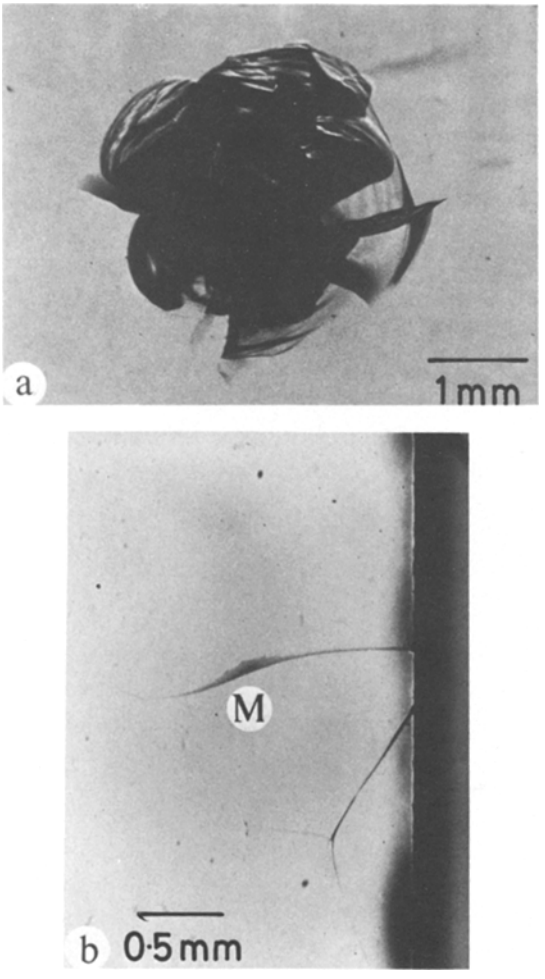

Figure 5 (a) Top view of the damage shown in Fig. 4. (b) View of the damage as revealed by sectioning parallel to the impacted surface. Note only one half of the damage is shown. The median crack is shown at M.

4. Fracture mechanics of the cracks

The fracture mechanics of the well-developed cone and the median cracks have been treated by Roesler [19] and Lawn and Fuller [20], respectively. In this paper we shall be concerned only with the median cracks produced by the pointed indenters/projectiles; an analysis of the cone cracks will be published elsewhere. The loading of the median cracks with the pointed indenters/projectiles can be likened to the loading of a disc-shaped crack in an infinite body by equal and opposite forces whose points of application are zero distance apart along the common line of action [21]. In the present case, this common

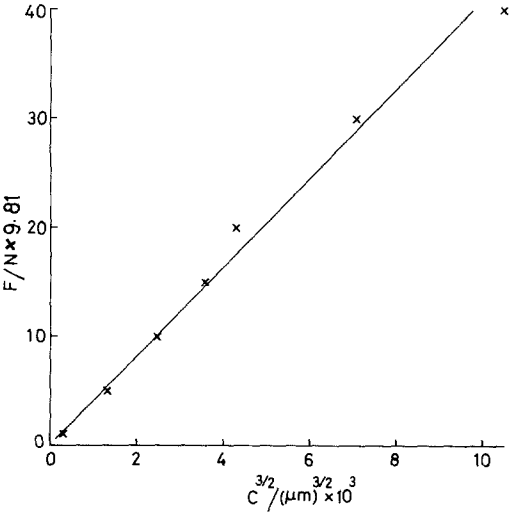

Figure 6 Plot of load versus (crack length)$^{3/2}$ for median cracks in fused silica produced by quasi-static loading with a Vickers diamond pyramid.

line of action is parallel to the indented/impacted surface and the magnitude of the individual force (considering the coefficient of friction between the surface of the indenter/projectile and the silica surface as zero) is $F/(2 \tan \theta)$ where θ is the semi-apical angle of the pyramid/cone and F the normal load on it. Neglecting the edge effects, the static stress intensity factory, K_s, for a crack of radius, C, is given by [21]

$$K_s = \frac{F}{2\beta_0 C^{3/2} \tan \theta}, \quad (1)$$

where $\beta_0 = \pi^{3/2}$.

5. Discussion

5.1. The inadequacy of the quasi-static approach

The time resolution (i.e. $1\,\mu\text{sec frame}^{-1}$) in our previous high-speed photographic investigations [1–3] was not able to reveal, but this higher time resolution (i.e. $0.6\,\mu\text{sec frame}^{-1}$) study has been, that the Hertzian cone crack (signifying the elastic regime) and the median crack (signifying the plastic/crushed regime) can also grow during the unloading part of the impact. Moreover the maximum crack velocity of the cracks in fused silica is found to be about 1.5 times that in soda-lime glass; under similar impact conditions the lengths of cone and median cracks in fused silica are considerably larger than those in soda-lime glass, whereas the situation is reversed in the quasi-static loading as mentioned in Section 3.3. Other notable factors are that in the impact case the strain rates are very high which can cause increases of yield stress [4] and brittleness.

On the basis of these observations it is clear that the size of a crack produced by the impact of a particle may be quite different from that produced by the quasi-static loading of the material to a load equivalent to the maximum load generated during the impact. Further evidence to support this view comes from our multiple impact experiments: similar impacts were made at a single site and it was found that the extent of the median and cone cracks increased with each individual impact, and approached a constant value for a sufficiently large number of impacts. According to the quasi-static approach, each impact produces the maximum force of the same magnitude. Therefore these results cannot be explained on the quasi-static theories. It seems possible that the crack growth is due to stress wave interactions which have not been considered in the previous treatments [8, 9].

5.2. A suggested approach

An alternative approach for predicting the extent of single-impact generated crack lengths is to consider the crack growth in terms of the dynamic stress-intensity factor and the crack velocity. But since the impact loading is of a short pulse type, the situation is complex and the analysis becomes very difficult. Some progress has, however, been made by Kalthoff and Shockey [22] for the simpler case of short square pulses and millimetre size cracks. Their analysis has shown that if the size of the cracks is $v_1 T/20$ or shorter, where v_1 is the velocity of the longitudinal wave in the material and T the duration of the pulse, then the dynamic stress-intensity factor is identical with the static stress-intensity factor for the duration of the pulse. Such conditions are approximately met in our experiments. According to our picture a crack will grow if the dynamic stress-intensity factor is greater than the critical value for the material under the prevailing dynamic conditions. It is easy to see, therefore, that the crack growth can also occur during the unloading part of the impact. The total crack length, C, in the impact case can be given by

$$C = \int_{t_0}^{t} V \, dt + C_0, \quad (2)$$

where t_0 is the time at which the crack of size C_0 is nucleated (critical loads for crack nucleation in static loading have been calculated by Hagan [23] and by Lawn and Evans [24], although at present no calculations exist for the dynamic case) and t is the time at which the crack comes to rest. But V is a function of the stress-intensity factor; this dependence can be obtained from these experiments (see below).

5.3. Stress-intensity factor of the high-velocity cracks

We shall first make an estimate of the resistance of fused silica to penetration by the impacting particles. For both spherical and conical particle impacts the material crushes during the early stages of loading and if we assume that the resistance remains constant at P, then the equation of motion of the particle (considered rigid) is

$$m\frac{d^2x}{dt^2} = \begin{cases} -2\pi rPx & \text{sphere} \\ -\pi Px^2 & \text{cone or semi-apical angle } \pi/4, \end{cases} \quad (3)$$

where x is the distance from the impacted surface, m the mass of the particle, r its radius, and t the time. The particle comes to rest at $x = x_0$, which by integration of Equation 3 is given by

$$x_0 = \begin{cases} \left(\frac{m}{\pi rP}\right)^{1/2} v_0 & \text{sphere} \\ \left(\frac{3m}{2\pi P}\right)^{1/3} v_0^{2/3} & \text{cone,} \end{cases} \quad (4)$$

where v_0 is the incident velocity. In the case of the sphere (Fig. 2) the maximum penetration of 150 μm occurs in frame 5. For $v_0 = 200\,\mathrm{m\,sec^{-1}}$, $r = 0.5$ mm, and particle density of $14.85\,\mathrm{Mg\,m^{-3}}$ we obtain the value of P as $8.8 \times 10^9\,\mathrm{N\,m^{-2}}$.

Using this value of P and $v_0 = 170\,\mathrm{m\,sec^{-1}}$, we predict from Equation 4 that the conical particle will penetrate to a maximum depth of 145 μm. The photographic sequence (Fig. 4) shows that the tip of the cone is into the material by 120 μm in frame 3; during the next 0.6 μsec the particle penetrates to the maximum depth, and starts to rebound, the governing equation being [25]

$$m\frac{d^2x}{dt^2} = -\pi Px^2\left(\frac{x - x_1}{x_0 - x_1}\right)^n \quad (5)$$

where x_1 is the depth of the residual indentation and n a free parameter given by

$$\left(\frac{v_e}{v_0}\right)^2 \simeq \frac{(3)}{(n+1)}\,\frac{(x_0 - x_1)}{(x_0)}, \quad (6)$$

in which v_e is the rebound velocity.

Unfortunately, because of the ejection of the crushed material, only rough measurements of the residual indentation could be made. From Equation 3 we get the loading time of $\sim 1.2\,\mu$sec, which is in agreement with the observed time of 1.2 to 1.8 μsec; the calculated unloading time is only a small fraction of 1 μsec.

Now we are in a position to make a rough estimate of the static equivalent of the dynamic stress factor, K_d, at different crack velocities from Fig. 4, and by using the calculated loads and the measured crack lengths. As the load increases between frames 1 and 2, plastic flow, crushing and median crack nucleation occurs. Although at present we do not know the size of the median crack at the instant of nucleation and the corresponding load, it is thought that the value of K_d is very high and this drives the crack at its maximum velocity. In frame 2 the value of K_d is $0.41 \times 10^6\,\mathrm{N\,m^{-3/2}}$, which drives the crack at a velocity of $1400\,\mathrm{m\,s^{-1}}$ between frames 2 and 3, whereas in frame 3 the value of K_d is $0.44 \times 10^6\,\mathrm{N\,m^{-3/2}}$ and the corresponding crack velocity is $950\,\mathrm{m\,sec^{-1}}$. One reason for this slight apparent inconsistency of slightly higher value of K_d but a smaller crack velocity is that complete unloading also occurs between frames 3 and 4. It is hoped that a more detailed behaviour of K_d versus V will be obtained using framing rates of 10^7 frames per second.

It is interesting to note that these values of K_d for which cracks move at a high velocity are considerably less than the value of $1.45 \times 10^6\,\mathrm{N\,m^{-3/2}}$ determined from static indentation experiments. Thus for high-velocity cracks the fracture surface energy ($\gamma \leqslant 1.1\,\mathrm{J\,m^{-2}}$) is considerably smaller than the value of $14.1\,\mathrm{J\,m^{-2}}$ obtained from the static indentations, and rather surprisingly it is about a half of the theoretically calculated value of $\sim 2\,\mathrm{J\,m^{-2}}$. This could be due to the inadequacies in the analysis and the calculated load–time behaviour of the impact. However, there is a definite trend towards a much smaller value of the fracture-surface energy for high-velocity cracks. Finally, in spite of any limitations in the analysis, experiments of the type reported here provide us with a potentially useful and simple method for determining the relationship between K_d and velocity of fast cracks from which the extent of cracks generated by a single impact can be predicted by using Equation 2. It must be emphasized that this approach is applicable to situations in which the crack lengths are within the limits imposed by the theory of Kalthoff and Shockey [22].

6. Conclusions

The high-speed photographic study has shown that the nature of the cracks formed by the impact of small spherical particles is different from those formed by pointed ones. Furthermore, contrary to the observations from static indentation experiments, growth of the Hertzian cone and median cracks can also occur during the particle rebound. Values of the static equivalent of the dynamic stress factor for high-velocity cracks have been found to be considerably smaller than those

obtained for the static indentation experiments, and a new approach for predicting the extent of cracks generated by single impacts has been suggested.

Acknowledgement

We would like to thank Dr J. T. Hagan for discussions and comments on the manuscript.

References

1. M. M. CHAUDHRI, C. G. KNIGHT and M. V. SWAIN, Proceedings of the 12th International Congress on High-Speed Photography, Toronto (Society of Photo-Optical Instrumentation Engineers, Washington, 1977) p. 371.
2. C. G. KNIGHT, M. V. SWAIN and M. M. CHAUDHRI, *J. Mater. Sci.* **12** (1977) 1573.
3. M. M. CHAUDHRI and S. M. WALLEY, *Phil. Mag.* **A37** (1978) 153.
4. M. M. CHAUDHRI and A. STEPHENS, Proceedings of the 13th International Congress on High-Speed Photography and Photonics, Tokyo (Japan Society of Precision Engineering, Tokyo, 1979) p. 726.
5. W. TAYLOR, *J. Soc. Glass Technol.* **34** (1950) 69.
6. T. O. MULHEARN, *J. Mech. Phys. Solids* 7 (1959) 85.
7. B. R. LAWN and T. R. WILSHAW, *J. Mater. Sci.* **10** (1975) 1049.
8. A. G. EVANS, *J. Amer. Ceram. Soc.* **56** (1973) 405.
9. S. M. WIEDERHORN and B. R. LAWN, *ibid* **60** (1977) 451; **62** (1979) 66.
10. F. M. ERNSBERGER, *ibid* **51** (1968) 545.
11. J. E. NEELY and J. D. MACKENZIE, *J. Mater. Sci.* **3** (1968) 603.
12. J. T. HAGAN, *ibid* **14** (1979) 642.
13. H. SCHARDIN, "Fracture", edited by B. L. Averbach, D. K. Felbech, G. T. Hahn and D. A. Thomas (Wiley, New York, 1959) p. 297.
14. J. E. FIELD, Ph.D dissertation, University of Cambridge (1962).
15. J. J. BENBOW, *Proc. Phys. Soc. London* **B75** (1960) 697.
16. J. T. HAGAN and M. M. CHAUDHRI, *J. Mater. Sci.* **12** (1977) 1055.
17. S. M. WIEDERHORN, *J. Amer. Ceram. Soc.* **52** (1969) 99.
18. K. KENDALL, *Proc. Roy. Soc. London* **A361** (1978) 245.
19. F. C. ROESLER, *Proc. Phys. Soc. London* **B69** (1956) 981.
20. B. R. LAWN and E. R. FULLER, *J. Mater. Sci.* **10** (1975) 2016.
21. P. C. PARIS and G. C. SIH, Amer. Soc. Test. Mater. Spec. Tech. Publ. No. 381 (1965) p. 30.
22. J. F. KALTHOFF and D. A. SHOCKEY, *J. Appl. Phys.* **48** (1977) 986.
23. J. T. HAGAN, *J. Mater. Sci.* **14** (1979) 2975.
24. B. R. LAWN and A. G. EVANS, *ibid* **12** (1977) 2195.
25. C. D. DAVIS and S. C. HUNTER, *J. Mech. Phys. Solids* 8 (1960) 235.

Received 13 June and accepted 2 July 1979.